Fatal outcome due to deficiency of subunit 6 of the conserved oligomeric Golgi complex leading to a new type of congenital disorders of glycosylation

Lübbehusen, Jürgen; Thiel, Christian; Rind, Nina; Ungar, Daniel; Prinsen, Berthil H C M T; de Koning, Tom J; van Hasselt, Peter M; Körner, Christian

Published in:
Human Molecular Genetics

DOI:
10.1093/hmg/ddq278

Document Version
Publisher's PDF, also known as Version of record

Publication date:
2010

Human Molecular Genetics, 2010, Vol. 19, No. 18 **3623–3633**
doi:10.1093/hmg/ddq278
Advance Access published on July 6, 2010

Fatal outcome due to deficiency of subunit 6 of the conserved oligomeric Golgi complex leading to a new type of congenital disorders of glycosylation

Jürgen Lübbehusen[1,†], Christian Thiel[1,†], Nina Rind[1], Daniel Ungar[2], Berthil H.C.M.T. Prinsen[3], Tom J. de Koning[4], Peter M. van Hasselt[4] and Christian Körner[1,*]

[1]Center for Child and Adolescent Medicine, Center for Metabolic Diseases Heidelberg, Department I, Im Neuenheimer Feld 153, D-69120 Heidelberg, Germany, [2]Department of Biology, University of York, PO Box 373, York YO10 5YW, UK and [3]WKZ Department of Metabolic and Endocrine Diseases and [4]Department of Metabolic Diseases, Wilhelmina Children's Hospital, University Medical Center Utrecht, Lundlaan 6, 3584 EA Utrecht, The Netherlands

Received May 4, 2010; Revised and Accepted June 30, 2010

Deficiency of subunit 6 of the conserved oligomeric Golgi (COG6) complex causes a new combined N- and O-glycosylation deficiency of the congenital disorders of glycosylation, designated as CDG-IIL (COG6-CDG). The index patient presented with a severe neurologic disease characterized by vitamin K deficiency, vomiting, intractable focal seizures, intracranial bleedings and fatal outcome in early infancy. Analysis of oligosaccharides from serum transferrin by HPLC and mass spectrometry revealed the loss of galactose and sialic acid residues, whereas import and transfer of these sugar residues into Golgi-enriched vesicles or onto proteins, respectively, were normal to slightly reduced. Western blot examinations combined with gel filtration chromatography studies in patient-derived skin fibroblasts showed a severely reduced expression of the mentioned subunit and the occurrence of COG complex fragments at the expense of the integral COG complex. Sequencing of *COG6*-cDNA and *COG6* gene resulted in a homozygous mutation (c.G1646T), leading to amino acid exchange p.G549V in the COG6 protein. Retroviral complementation of the patients' fibroblasts with the wild-type *COG6*-cDNA led to normalization of the COG complex-depending retrograde protein transport after Brefeldin A treatment, demonstrated by immunofluorescence analysis.

INTRODUCTION

'Protein glycosylation' describes the co-translational linkage and modification of oligosaccharide moieties on newly synthesized proteins. This complex metabolic process, which has been found in nearly all forms of life from bacteria to man, comprises one of the most widespread and variable forms of protein modifications. Owing to their structural variability, glycans are carriers of a code that is much more complex compared with nucleic acids and proteins. Glycoproteins play an important role in many biological processes such as growth, differentiation, organ development, signal transduction and immunologic defence, but are also involved in pathologic processes like tumour progression (1,2). The N- and O-glycosylation machinery is addicted to an interaction of a bulk of proteins located in the cytosol, endoplasmic reticulum and the Golgi apparatus. Inborn errors in the glycosylation process in man are termed 'congenital disorders of glycosylation' (CDG). They comprise a rapidly expanding group of autosomal recessive inherited metabolic diseases, presenting mostly with a multisystemic phenotype combined with severe neurological impairment. In recent years, not only defects in distinct glycosyltransferases, glycosidases or nucleotide-sugar transporters have been identified, but also deficiencies in the supply of products or in the maintenance of a correct pH value, all necessary for the proper proceeding of protein glycosylation, have been described (3–5). Furthermore, several defects in different subunits of the conserved oligomeric Golgi (COG) complex have been identified (3). The COG complex is a hetero-octameric protein complex

*To whom correspondence should be addressed. Tel: +49 6221562881; Fax: +49 6221565907; Email: christian.koerner@med.uni-heidelberg.de
†The authors wish it to be known that, in their opinion, the first two authors should be regarded as joint First Authors.

(6–9) in the cytosol which is associated with the Golgi apparatus and is required for proper sorting and glycosylation of Golgi-resident enzymes and secreted proteins. Thereby, it is involved in the retrograde transport by COPI vesicles and assumes a role as tethering factor for initial interactions of vesicles with the target membrane (9–11). Recent studies on the COG complex structure in CDG patients let assume a subunit interaction of COG2–COG4 and COG5–COG7 which form lobes A and B, respectively, that are connected by COG1 and COG8 (6,9). Dysfunction of the COG complex leads to a generalized hypoglycosylation in the cells ending up in a severe clinical phenotype of the affected patients. Since 2004 deficiencies in subunits COG7 (12), COG1 (13), COG8 (14,15), COG4 (7) and COG5 (8) of the hetero-octameric COG complex have been shown to lead to its malfunction and subsequently to hypoglycosylation of glycoproteins and therefore to CDG. Here, we present a new type of the CDG by identification of the molecular defect in a patient with deficiency of subunit 6 of the COG complex.

RESULTS

Case report

The index patient was the fourth child of healthy non-consanguineous parents of Turkish origin. The family history included two other children that died in the perinatal period (one shortly after delivery and the other at 5 weeks of age) with signs of an increased bleeding tendency. Pregnancy and delivery of the female patient were uncomplicated and at term. The patient suffered from intractable focal seizures, vomiting and loss of consciousness due to intracranial bleedings. Biochemical investigations revealed a normal level for albumin and mildly elevated values for lactate, aspartate aminotransferase and creatine kinase. Metabolic investigations revealed cholestasis and subsequent vitamin K deficiency, explaining in part her intracranial bleedings. The patient died due to brain oedema at 5 weeks of age. Since the clinical phenotype of the patient was suspect for a CDG syndrome, initial CDG diagnosis was established by isoelectric focusing (IEF) of the patient's serum transferrin.

Analyses of serum transferrin, α-1-antitrypsin and apolipoprotein CIII

Diagnosis of CDG was performed by IEF and western blotting of serum transferrin. The IEF pattern from the CDG-IIL patient showed the presence of transferrin molecules with four, three, two, one or no sialic acid residues (Fig. 1A), typical for CDG-type II deficiencies. The partial loss of sugar residues of *N*-glycans in CDG-IIL was demonstrated by a smear in western blotting of serum transferrin (Fig. 1B) in contrast to a control or a CDG-Ia patient, who showed defined additional bands with faster mobility due to the complete loss of either one or two glycan chains, typical for CDG-I deficiencies. To confirm CDG in the patient, IEF of an alternative glycoprotein, plasma α-1-antitrypsin, was performed. Human plasma α-1-antitrypsin is normally glycosylated at amino acid residues 46, 83 and 247. Owing to the combinations of tri- and di-antennary-complex-type oligosaccharides and shortened isoforms of the protein, a pattern of seven bands in the IEF analysis of α-1-antitrypsin in healthy controls (Fig. 1C, lane 1) is detectable. For CDG, it has been shown that additional bands with a cathodal shift appear, the number and the size of which depend on the corresponding type of CDG (Fig. 1C, lanes 2 and 3). To further investigate, if the patient's defect also has an impact on the biosynthesis of core 1 mucin type O-glycans, IEF of the corresponding marker protein apolipoprotein CIII (ApoCIII) derived from sera of the patient and a control was performed. This method allows the quantitative determination of the three ApoCIII isoforms ($ApoCIII_{0-2}$), either with two sialic acid residues in 2,3 and 2,6 orientation ($ApoCIII_2$), with one sialic acid residue in 2,3 or 2,6 orientation ($ApoCIII_1$) or with no sialic acid residue ($ApoCIII_0$). In the case of the patient, an increased $ApoCIII_0$ pattern was detected. This difference in charge could be induced by a hypoglycosylation of the glycan or a mutation in the backbone of the protein. To find out, treatment of the patient's and a control serum with a 2,3-sialidase and an unspecific cutting sialidase was accomplished. Sialidase treatment with the 2,3-sialidase revealed disappearance of the fully sialylated $ApoCIII_2$ form in the case of the control and the patient. Where in the control, the ratio of $ApoCIII_1$ to $ApoCIII_0$ was balanced, the patient showed minor $ApoCIII_1$. Incubation with the unspecific cutting sialidase led to the emergence of $ApoCIII_0$ by deprivation of $ApoCIII_1$ and $ApoCIII_2$ forms in control and the patient. These results indicated a combined N- and O-glycosylation deficiency in the patient.

Lectin staining with peanut agglutinin

Staining of control and patient's fibroblasts with biotinylated peanut agglutinin (PNA) revealed enhanced binding of the lectin to the patient cells (data not shown). Since PNA binds specifically to galactose-β-(1-3)-*N*-acetylgalactosamine O-glycans, our result pointed to an O-glycosylation defect in the case of the patient by indicating loss of terminal sialic acid residues that prevents binding of PNA in the case of the control.

Analysis of transferrin-linked *N*-glycans

To further investigate the transferrin-linked oligosaccharides of the patient, transferrin was purified from control and patient's serum. Oligosaccharides were released with peptide-N-glycosidase F and reductively aminated with the fluorophore 2-AB. Fractionation by HPLC showed that the main glycan peak of the control co-eluted with a 2-AB-$GlcNAc_2Man_3$-$GlcNAc_2Gal_2Neu(N)Ac_2$ standard oligosaccharide at 49 min (Fig. 2). In the case of the patient beyond this full-length complex type *N*-glycan, several other oligosaccharides eluted earlier (peaks at 29, 34, 39, 41 and 44 min; Fig. 2) than those from control transferrin. This suggested that oligosaccharides of the patient were smaller in size. Matrix-assisted laser desorption/ionization–time of flight (TOF) analysis revealed, for the major oligosaccharide from control and the patient's transferrin (peak at 49 min), a mass of 2343.81 Da, which corresponds to 2-AB-$GlcNAc_2Man_3GlcNAc_2Gal_2Neu(N)Ac_2$. Other isolated oligosaccharides from the patient's transferrin revealed masses of 1437.32 Da (29 min), 1599.35 Da

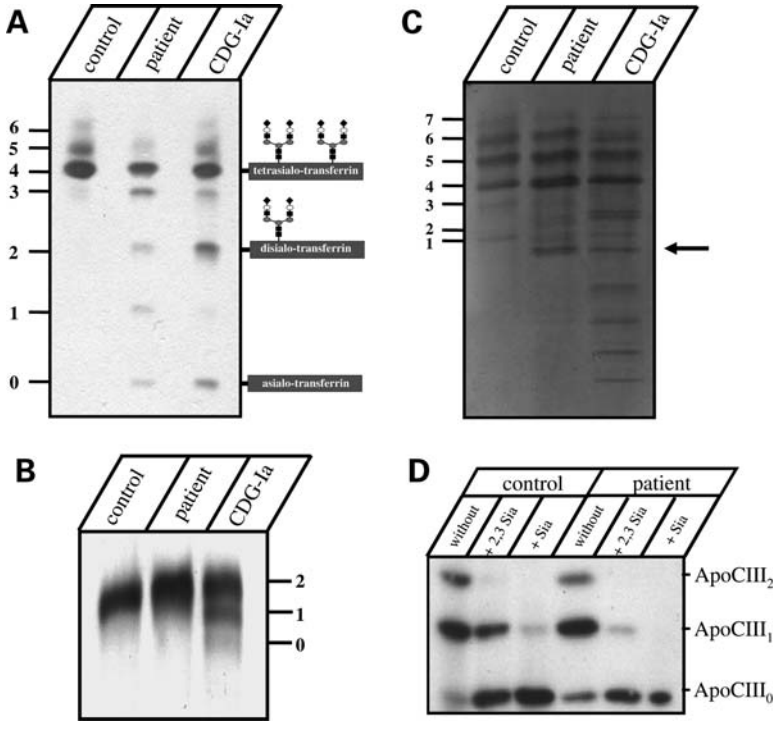

Figure 1. (**A**) Serum samples from a control (lane 1), a CDG-Ia reference patient (lane 3) and the patient (lane 2) were investigated by IEF, followed by in gel immunodetection of transferrin. Asialo, disialo and tetrasialo indicate transferrin forms carrying either 0, 2 or 4 sialic acid residues. (**B**) Shown are serum samples from a control, a CDG-Ia reference patient and the patient analysed by SDS–PAGE, followed by western blotting and immunodetection of transferrin. 0, 1 and 2 indicate transferrin forms carrying 0, 1 or 2 *N*-glycans. (**C**) IEF pattern of α-1-antitrypsin. Sera from a control (lane 1), the patient (lane 2) and a CDG-Ia patient (lane 3) were analysed by IEF. The normal pattern (lane 1) reveals seven bands. In abnormal patterns (lanes 2–3), the position of the first additional abnormal cathodal band is indicated by an 'arrow'. This band and all bands below are abnormal and indicate a glycosylation deficiency. (**D**) Analysis of core-1 mucin-type O-linked glycans derived from ApoCIII. Serum-derived ApoCIII from a control (lanes 1–3) and the CDG-IIx patient (lane 4–6) was investigated by IEF followed by antibody staining with a polyclonal rabbit-α-human ApoCIII antibody. $ApoCIII_2$, $ApoCIII_1$ and $ApoCIII_0$ indicate the variability in the amount of sialic acid residues linked to ApoCIII.

(34 min), 1761.15 Da (39 min), 1890.74 Da (41 min), 2052.75 Da (44 min) and 2343.81 Da (49 min). The loss of two sialic acid residues and two galactose residues accounts for the difference between 2343.81 and 1437.32 Da. The mass of 1599.35 Da from the second oligosaccharide corresponds to a structure with no sialic acid residue and only one galactose residue. By loss of both sialic acid residues, a mass of 1761.15 Da would be expected. The oligosaccharide that eluted at 41 min showed a mass of 1890.74 Da, indicating the loss of one sialic acid residue and one galactose residue. The fifth oligosaccharide with a mass of 2052.75 Da corresponds to 2-AB-$GlcNAc_2Man_3GlcNAc_2Gal_2Neu(N)Ac_1$. However, also full-length N-linked oligosaccharides were detected. Our results demonstrate that the N-linked oligosaccharides on the patient's transferrin have a complete or partial loss of galactose and neuraminic acid residues.

Determination of UDP-galactose and CMP-NANA import and measurement of galactose and sialic acid residues transfer

Since our findings on transferrin-linked *N*-glycans mentioned above could be explained by a deficiency of the import of UDP-galactose into the Golgi or by a reduced transfer of galactose residues to the glycoprotein, we determined the import of UDP-galactose and the activity of β-1,4-galactosyltransferase in control and patient-derived fibroblasts. Normal values for the UDP-galactose import (98% ± 6) in combination with a slightly decreased activity of β-1,4-galactosyltransferase (76% ± 5) were detected for the patient in comparison to the control. Besides, the import of CMP-NANA (70% ± 11) and the transfer of sialic acid residues (58% ± 4) were decreased (Fig. 3).

Western blotting of the COG complex subunits

Since combined N- and O-glycosylation diseases have been described in recent years for different defective subunits of the COG complex, analyses of the expression levels of COG1, COG4, COG5, COG6 and COG7 were performed from the patient fibroblasts and normalized against the expression of control fibroblasts. Equal amounts of protein were used for the assays, as has been proved by β-actin staining. In contrast to COG1 (97% ± 5) and COG4 subunits (100% ± 2), reduced signals of protein were detected for COG5 (55% ± 7), COG6 (21% ± 8) and COG7 (62% ± 4) in the case of the patient (Fig. 4A).

Northern blotting

To investigate, if the reduced amount of COG6 detected for the patient in western blotting was due to a decreased translation or successive degradation processes of the *COG6*-mRNA or due to

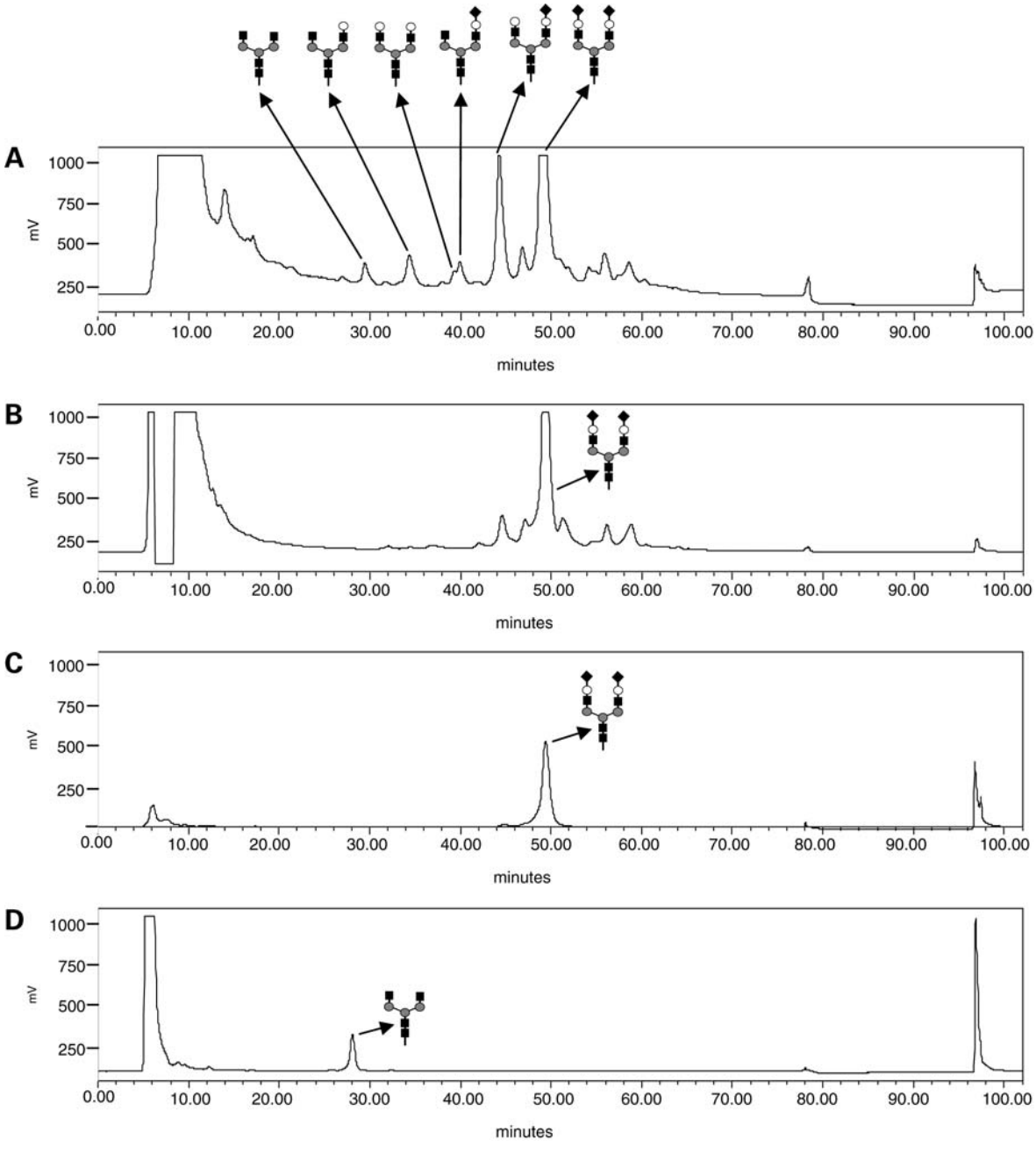

Figure 2. HPLC and mass spectrometric analysis of transferrin-linked oligosaccharides. Transferrin was purified from the serum of a control and the patient. Oligosaccharides were released by PNGase F digestion and subsequently analysed by HPLC (A patient, B control, C standard A2-2AB, D standard NGA2-2AB). The peak fractions were further investigated by mass spectrometry. The symbols over the HPLC peaks indicate the detected oligosaccharides. Symbols: squares, *N*-acetylglucosamine; grey circles, mannose; white circles, galactose; diamonds, neuraminic acid.

a reduced expression, we performed northern blot analysis for *COG6* and *β-actin*. In the case of the patient, a reduced signal for *COG6* to 16% $\pm$ 4 was identified in comparison to the control (Fig. 5), indicating that the decreased amount of COG6 protein was provoked by the instability of the patient's *COG6*-mRNA and not by degradation of the mutated protein. Hybridization with a probe specific for *β-actin* showed that equal amounts of the control and the patient's total RNA were used for the test. Since western and northern blot analyses both hint at a deficiency of COG6 or of one of the other subunits in the respective COG complex lobe in the case of the patient, further investigations were performed by mutational analyses on RNA and DNA levels.

Genetic analysis

In the case of the patient, sequencing analyses of the cDNAs for *COG5*, *COG7* and *COG8* were negative. Sequencing analysis of the *COG6*-cDNA revealed in the case of the patient a homozygous mutation (c.G1646T), leading to

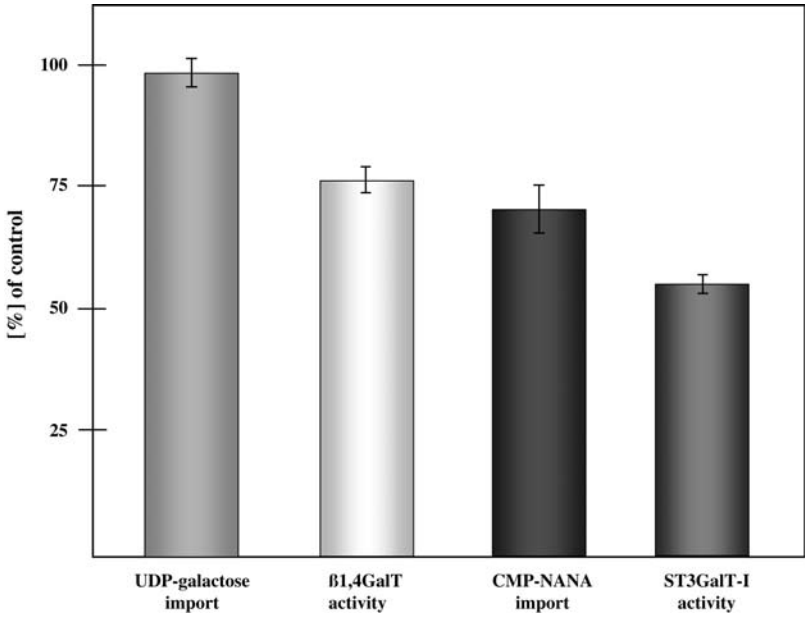

Figure 3. UDP-[6-^{3}H]galactose and CMP-[^{14}C]NANA import into microsomes, activity of β1,4GalT1 and transfer of sialic acid onto glycoproteins of the patient were measured and normalized to controls. Shown are data of three unrelated experiments.

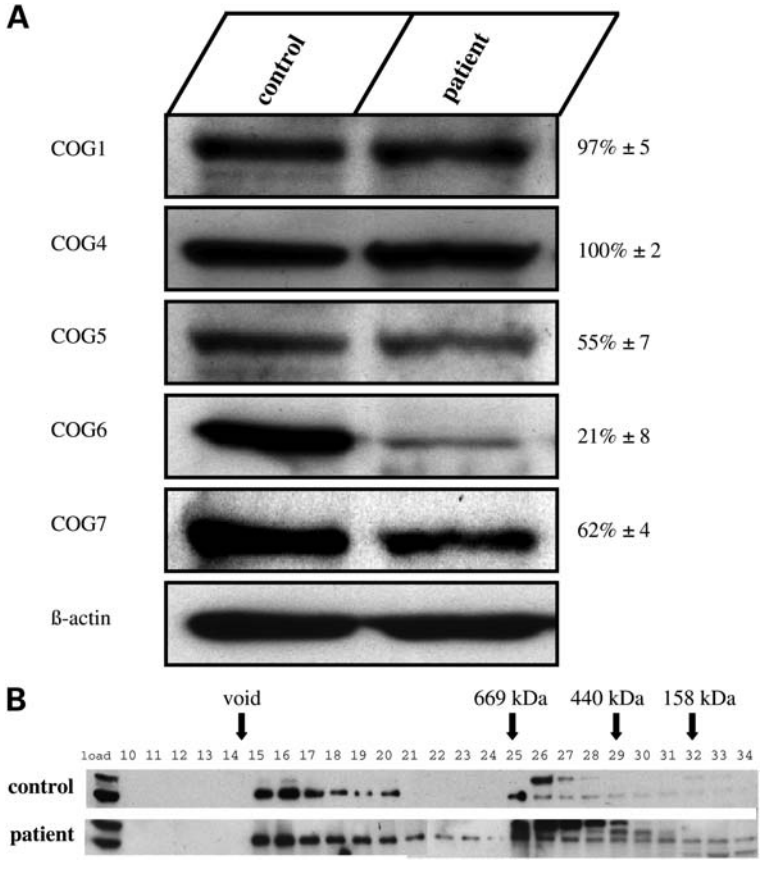

Figure 4. (**A**) Expression of COG1, COG4, COG5, COG6 and COG7 in control and patient-derived fibroblasts was analysed by western blot. The relative signal intensity of the respective subunit is shown as midpoint ± standard deviation ($n = 4$) and referred to β-actin and the signal intensity of the control. (**B**) Gel filtration chromatography of the COG complex. Cell lysates of fibroblasts of a control and the patient were separated by gel filtrations and analysed by western blot with an antibody against COG4. Specified above are weights of protein standards thyroglobulin (669 kDa), ferritin (440 kDa) and aldolase (159 kDa) plus the void volume.

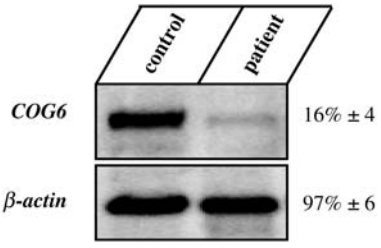

Figure 5. Northern blot analysis for *COG6*. Total RNA was isolated from a control and the patient and hybridized with a *COG6*-specific probe. Subsequently, hybridization with a probe specific for *β-actin* was performed to normalize the data.

amino acid exchange p.G549V in the COG6 protein. Sequence analysis of genomic DNA confirmed the mutational status of the patient. In 100 control alleles, this mutation has not been found (data not shown).

Gel filtration chromatography

To further investigate a potential impact of mutation p.G549V on the constitution of the COG complex, cell lysates of control and patient-derived fibroblasts were separated by gel filtration chromatography, fractionated and subsequently analysed by western blot with an antibody against COG4. In the case of the control, signals for the COG4 antibody were mainly detected in fractions 15–20, corresponding to a mass of ~800 kDa, which would match the entire COG complex. Additional signals were observed from fraction 25 to fraction 34 that became weaker with time. Strong signals in fractions 26 and 27 (upper band) were due to unspecific binding of the antibody. In the case of the patient fibroblasts, signals were detected throughout fractions 15–34 when incubated with the COG4 antibody. In contrast to the control, the patient showed more signals in fractions of smaller masses (Fig. 4B).

Complementation of COG6 deficiency in CDG-IIL fibroblasts

In order to confirm the deficiency of COG6 as cause for the glycosylation defect of our patient, we expressed the wild-type *COG6*-cDNA in patient's fibroblasts, utilizing retroviral gene transfer. As a control, we investigated whether the retroviral vector alone affects the functionality of the COG complex in the patient-derived fibroblasts by retrograde protein transport studies after Brefeldin A (BFA) treatment. BFA is widely used to investigate the function of the Golgi apparatus and the mechanisms regulating membrane trafficking in different cell types.

By reversible interaction with the GDP/GTP-exchange factor, BFA inhibits the activation of ADP-ribosylation factor 1, and thereby interfering with elementary procedures in the Golgi. Moreover, BFA inhibits the formation of COPI vesicles on the Golgi apparatus, necessary for the anterograde protein transport. Since the retrograde transport of proteins is not affected by BFA treatment, incubation with BFA leads to a rapid relocation of Golgi proteins into the endoplasmic reticulum and subsequently to the disorganization of Golgi compartments (16). As in cases of different COG deficiencies, a significant delay in the breakdown of Golgi compartments was noticed after BFA treatment, fibroblasts of a control and our patient were incubated with BFA for different periods (0–15 min) and analysed for their Golgi structures by immunofluorescence studies with the Golgi marker GM130 (Fig. 6A–P) after proving that GM130 and COG4 co-localize (data not shown). Quantification of control and patient's fibroblasts was performed by analysing the ER staining pattern of 300 cells at different time points, respectively (Table 1). Non-transduced control (Fig. 6A) and patient-derived fibroblasts (Fig. 6E) as well as mock-transduced (Fig. 6I) and wild-type COG6-transduced fibroblasts (Fig. 6M) of the patient showed the localization of GM130 in all cisterns of the Golgi apparatus at time point 0 min. In the case of the control, degradation of the Golgi compartments was completed after 5 min incubation with BFA (Fig. 6B), where in the case of the non-transduced (Fig. 6H) and mock-transduced (Fig. 6L) fibroblasts of the patient, the same effect was not visible before 15 min. After retroviral transduction of patient-derived fibroblasts with wild-type *COG6*-cDNA, a 5-min incubation with BFA was sufficient for a nearly complete redistribution of Golgi proteins and therefore comparable to the non-transduced control (Fig. 6N).

DISCUSSION

In a patient who presented clinically with a multi-organic phenotype characterized by intractable focal seizures, vomiting and loss of consciousness due to intracranial bleedings and death in early infancy, we identified the deficiency of COG6 complex as a molecular cause for her disease.

Initial diagnostics for the glycosylation state of the patient's serum transferrin led to a characteristic CDG-II pattern. The result was confirmed by IEF of the alternative marker protein α-1-antitrypsin as well as by western blot analysis of serum transferrin. Investigation of ApoCIII by IEF further showed that also core 1 mucin-type O-glycans were affected in the case of the patient, which accordingly led to an enhanced staining pattern with lectin PNA. The data clearly indicated a generalized defect in protein N- and O-glycosylation. Since mass spectrometric investigations of the patient's transferrin bound *N*-glycans additionally revealed a decrease in galactosylation and sialylation with all forms from agalacto- (2-AB-$GlcNAc_2Man_3GlcNAc_2$) to disialotransferrin (2-AB-$GlcNAc_2Man_3GlcNAc_2Gal_2Neu(N)Ac_2$) combined with the reduced activities of UDP-galactose and CMP-NANA transporters as well as of β1,4GalT1 and ST3GalTI glycosyltransferases, our data indicated comparability in essential biochemical hallmarks known for the COG complex diseases (6). To date, five defects in different subunits of the COG complex have been associated with CDG: COG7 (12), COG1 (13), COG8 (14,15), COG4 (7) and COG5 (8). The clinical picture of the COG defects ranges from mildly (in the case of COG5) to severely affected with death in early infancy (in the case of COG7 and COG6). Nevertheless, due to the small amount of COG patients identified so far, the informative value is still limited. In general, these patients suffer from growth retardation, failure to

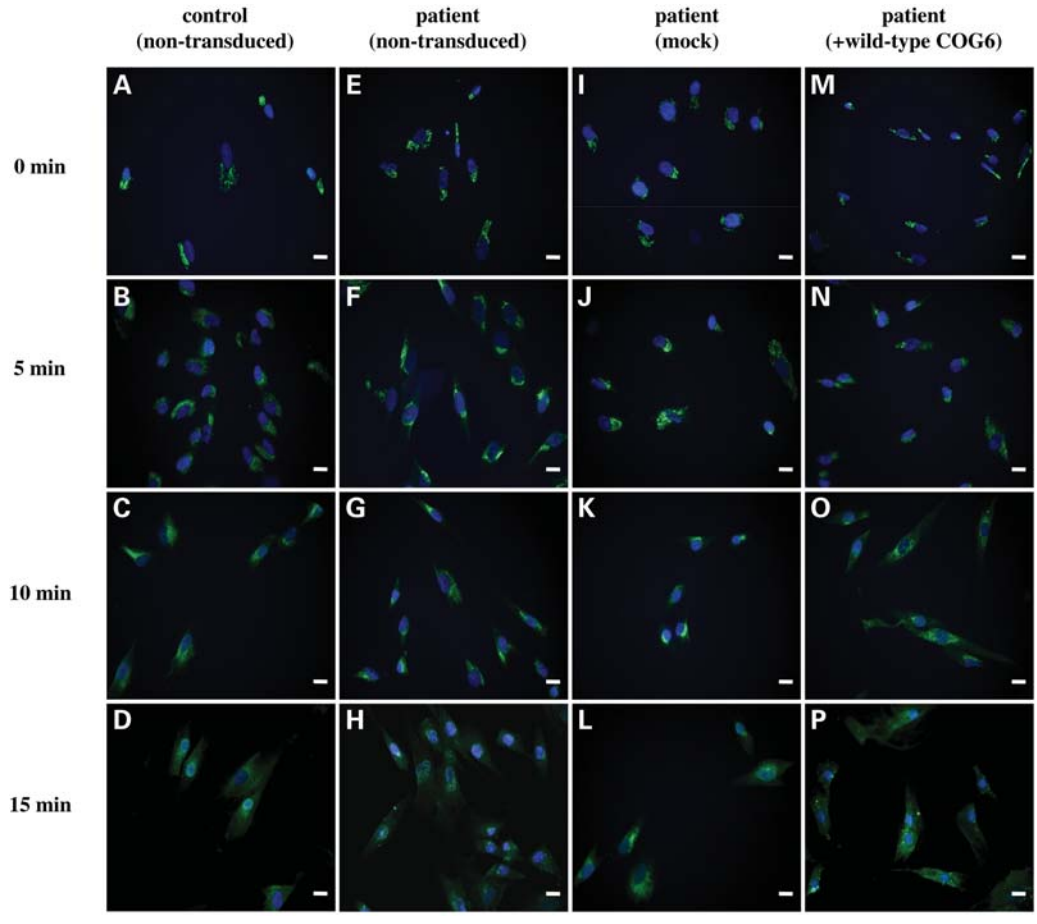

Figure 6. BFA assay. Fibroblasts of a control (non-transduced, **A**–**D**) and the patient (non-transduced, **E**–**H**; mock-transduced, **I**–**L**; wild-type COG6 transduced, **M**–**P**) were incubated for different periods (0–15 min) with BFA. Cells were fixed and analysed by immunofluorescence for localization of Golgi marker GM130 (green). The cell nucleus (blue) was stained with DAPI. Bar: 10 μm.

thrive, hypotonia, microcephaly and cerebral atrophy, features which are also known from other glycosylation deficiencies of CDG-I and CDG-II.

Besides the biochemical characteristics mentioned above, COG patients show instability of their affected COG complex subunit(s). Hence, we analysed the steady-state levels of the COG proteins of our patient by western blotting and found clearly reduced amounts of the patient's COG6 (minus ∼78%), COG5 (minus ∼44%) and COG7 (minus ∼38%) in comparison to the control, assuming an affection of its COG complex lobe B. This is consistent with recent findings in other COG patients, where mutations in one of the COG subunits caused protein instability which was always accompanied by reduced expression of at least one other subunit of the respective lobe. Sequencing analyses of *COG5*- to *COG8*-cDNAs revealed a homozygous mutation (c.G1646T) in the *COG6*-cDNA of the patient that caused amino acid exchange p.G549V. In contrast to other COG patients, this mutation did not lead to reduced amounts of COG6 by protein instability or degradation, rather instability of the patient's *COG6*-mRNA occurred, as has been demonstrated by northern blot analysis. By gel filtration chromatography combined with western blotting for the detection of subunit COG4, we investigated the effect of the reduced COG6 level on the patient's COG complex structure (Fig. 4B). Main signals were detected in fractions 15–20 in the case of the control, indicating the presence of the entire COG complex with a size of ∼800 kDa. Further diminishing signals with masses between protein standards thyroglobulin (669 kDa) and aldolase (158 kDa) were observed from fraction 25 on, which could be explained by the existence of COG subcomplexes (e.g. COG1 to COG4 plus COG8 with a mass of ∼460 kDa or COG5 to COG8 with a mass of ∼340 kDa), since similar effects were also observed in different COG-deficient mammalian cell lines (17). In the case of the patient, signals indicating the full COG complex were seen in fractions 15–20, leading to the assumption that the mutated COG6 subunit allows for the assembly of the complete COG complex. Nevertheless, in contrast to the control, more signals in fractions 21–34 in the patient-derived fibroblasts with masses smaller than 700 kDa were detected, which might be ascribed to the accumulations of COG subcomplexes. As also signals in fractions 32–34 were observed, there is incidence for the existence of subunit COG4 with another subunit of lobe A or with COG1 as

Table 1. Quantification of control and patient-derived fibroblasts after incubation with BFA

Incubation time (min)	Control (non-transduced) (%)	Patient (non-transduced) (%)	Patient (mock) (%)	Patient (+WT COG6) (%)
0	0	0	0	0
5	95	10	14	93
10	100	81	86	94
15	100	98	93	100

Shown are percentage of cells with ER staining pattern at the respective time points.

well as COG4 protein on its own, suggesting a complete breakdown of the patient's COG complex in part. If this was due to the decrease in the steady-state level of COG6 protein in combination with down-regulations of its partners COG5 and COG7, which might result in a lower association of all subunits with the Golgi compartments or due to a direct impact of mutation p.G549V on the patient's COG complex structure itself, remains to be solved. However, glycine 549 seems to play an important role in COG6 function, since it is a highly conserved amino acid residue in COG6 proteins from yeast to man. To find out if functionality of the patient's COG complex is affected, BFA treatment was performed. As has been demonstrated for deficiencies of COG7 (18), COG8 (14,15), COG4 (7) and COG5 (8), treatment of the respective patient cells with BFA led to a prolonged disintegration of the patients Golgi compartments. In the case of our patient, BFA treatment of the fibroblasts led to a 3-fold time delay in retrograde transport of Golgi-resident proteins in comparison to the control, evidencing a malfunction of the patient's COG complex. After retroviral transduction of the wild-type *COG6*-cDNA into the patient's cells, functionality of its COG complex could be reassembled to a control-like rate, whereas transduction with the empty vector (mock) led to no effect, proving that the depletion of subunit COG6 was disease-causing in our patient.

Recent experiments from yeast presumed that the deletion of SEC37, the corresponding subunit to human COG6, neither interferes with cell growth nor indicates that the association of the COG core proteins (COG1–COG4) has been affected (19,20) which is consistent with data from *Caenorhabditis elegans* where mutations in the COG subunits of lobe A lead to a more severe phenotype than those occurring in lobe B of the *C. elegans* complex (9). After identification of a disease-causing mutation in subunit COG7 (12), the COG6 deficiency described here is the second defect with fatal outcome after a few weeks of life. Since both subunits are the members of the COG complex lobe B, the allocation of essential and non-essential subunits of the human COG complex is therefore not compatible with the dispositions of subunits from the COG complexes of other species. As also deficiencies of COG2 and COG3 of lobe A have to be identified in patients, the concluding consideration on the role of the different human COG complex subunits remains to be solved.

MATERIALS AND METHODS

Cell lines and cell culture

Fibroblasts from the index patient and controls were maintained at 37°C under 5% CO_2 in Dulbecco's modified Eagle's medium (DMEM, Invitrogen), which contained 10% fetal calf serum (FCS; PAN Biotech GmbH), 50 IU/ml penicillin and 50 μg/ml streptomycin. The ecotropic packaging cell line FNX-Eco (ATCC) and the amphotropic packaging cell line RetroPack PT67 (Clontech) cultured in DMEM containing 1× L-glutamine, 1× Pen/Strep and 10% fetal calf serum (PAN Biotech GmbH), which was heat inactivated at 56°C for 30 min, at 37°C under 5% CO_2 unless otherwise stated.

Antibodies

For western blot analyses, the primary antibodies rabbit antihuman ApoCIII (Biotrend, Cologne), the COG complex subunits COG1, COG4, COG5, COG6 and COG7 (D. Ungar), human serum transferrin (DakoCytomation) and α-1-antitrypsin (DakoCytomation) were used in dilutions of 1:1000 in PBST (0.1% Tween-20), respectively. Primary antibodies mouse antihuman β-actin (Sigma-Aldrich) and mouse antihuman GM130 (Sigma-Aldrich) were used in dilutions of 1:10 000 in PBST and 1:200 in PBS, respectively. Secondary antibody goat anti-rabbit labelled with horseradish peroxidase (Dianova) was used in a dilution of 1:10 000 in PBST. Fluorochrome-conjugated secondary antibody goat anti-mouse Alexa488 (Invitrogen) for the detection of human GM130 was diluted 1:400 in PBST.

IEF and western blot analyses of serum transferrin

IEF and western blot analyses of serum transferrin were performed as described previously (21).

IEF of α-1-antitrypsin

IEF of human α-1-antitrypsin was performed as described (22).

IEF of ApoCIII

IEF of ApoCIII was performed as described (23).

Neuraminidase treatment

Desialylation of glycopeptides of a control and the patient was performed with two different neuraminidases, respectively. 2,3-neuraminidase (Takara) cuts sialic acid residues attached to galactose residues in 2,3 orientation, whereas neuraminidase isolated from *Vibrio cholerae* (Roche) cuts 2,6-linked sialic acid residues from *N*-acetylgalactosamine acids and 2,3-linked sialic acids residues from galactose residues. For the assay 12.5 μl serum, 2.5 μl of 1 M NaAc (pH 5.0), 9.5 μl water and 1 μl (0.01 U) of the respective enzyme were incubated at 37°C for 4 h. One microlitre was used for IEF of ApoCIII.

Analysis of transferrin-linked *N*-glycans

Oligosaccharide moieties of a control and the patient's serum transferrin were isolated, purified and analysed by mass spectrometry on a Bruker Ultraflex TOF/TOF as described previously (24).

Histochemical staining with PNA

Control and patient-derived fibroblasts were stained with 2 μg/ml biotinylated PNA (Vector Laboratories) in PBS/1% BSA (Sigma-Aldrich) as described (25).

Analysis of UDP-[6-^{3}H]galactose and CMP-[^{14}C]NANA import

The import of UDP-[6-^{3}H]galactose (Perkin Elmer) and CMP-[^{14}C]NANA (Perkin Elmer) into Golgi-enriched vesicles from control and patient's fibroblasts was assessed as described previously (26).

Analysis of UDP-galactose:*N*-acetylglucosamine β-1,4-galactosyltransferase I activity and transfer of CMP-[^{14}C]NANA onto glycoproteins

The activity of the UDP-galactose:*N*-acetylglucosamine β-1,4-galactosyltransferase I (β1,4GalTI) was determined as described (24). Activity of the CMP-*N*-acetylneuraminate-β-galactosamide-α-2,3-sialyltransferase (ST3GalTI) was determined analogous to the β1,4GalTI measurement by following the transfer of 0.06 μCi CMP-[^{14}C]NANA (Perkin Elmer) onto acceptor protein asialofetuin type I (Sigma-Aldrich).

Western blot analyses of the COG subunits

Patient and control fibroblasts were lysed in TBS/1% Triton X-100/protease inhibitor mix (Serva) for 30 min on ice, followed by sonification and vortexing. After centrifugation (16 100 *g*, 4°C for 20 min), 30 μg protein of the supernatant was separated on a denaturing 10% SDS–polyacrylamide gel and transferred onto a nitrocellulose membrane by semi-dry western blotting. The membrane was blocked with 5% milk powder in PBST for 1 h at room temperature (RT) and incubated with antibodies against COG1, COG4, COG5, COG6 and COG7 as well as against β-actin in PBST overnight at 4°C. The membrane was washed three times with PBST for 20 min at RT and incubated with the secondary HRP-coupled antibody for 1 h at RT. After washing, visualization was performed by adding chemiluminescent reagent (Pierce).

Sequencing analyses

Total RNA was extracted from controls and patient-derived fibroblasts using the RNAeasy kit (Qiagen). First-strand cDNA was synthesized from 0.5 μg of total RNA with Omniscript reverse transcriptase (Qiagen) and primer COG6-R1. COG6 cDNA was amplified with primers COG6-F1 and COG6-R1 with the HotStar-*Taq*-Polymerase kit (Qiagen) with a preincubation at 95°C for 15 min followed by 30 cycles with 1 min at 94°C, 0.5 min at 55°C and 4 min at 72°C. The nested PCR with 35 cycles was carried out with the primers COG6-F2 and COG6-R2. Reverse transcriptase–PCR products were analysed on 1% agarose gels. PCR fragments were prepared with the QIAquick PCR purification kit (Qiagen) and subcloned into the pGEM-T-easy vector (Promega). Genomic DNA was prepared from control and patient-derived fibroblasts by the standard procedures (27). In a first round of PCR, exon 2 of the *COG6* gene was amplified from 100 ng template with primers COG6-Ex2-F1 and COG6-Ex2-R1 using the *Pfu*-TurboTaq-Polymerase (Stratagene) with a preincubation at 95°C for 1 min followed by 28 cycles with 1 min at 94°C, 0.5 min at 55°C and 1 min at 72°C. Further amplification was carried out with nested primers COG6-Ex2-F2 and COG6-Ex2-R2. PCR products were analysed on a 1% agarose gel, extracted with the QIAquick PCR purification kit (Qiagen). Sequence analysis of PCR products and plasmids was performed by dye-determined cycle sequencing with primers COG6-F2, COG6-F3, COG6-F4, COG6-F5 and COG6-R2 for COG6-cDNA and with COG6-Ex2-F2 and COG6-R2 for exon 2 of *COG6* gene on a Applied Biosystems model 373A automated sequencer. Analyses of the *COG5*-, *COG7*- and *COG8*-cDNAs from the patient and controls were performed accordingly to the protocol for *COG6* mentioned above. Primers for PCR amplifications and sequencing are listed in Table 2.

Northern blotting

Northern blotting was carried out for *COG6* and *β-actin* by following the standard procedures (27) with 5 μg of total RNA extracted from controls and patient-derived fibroblasts using the RNAeasy kit (Qiagen). RNA was transferred onto a nylon membrane (Amersham Hybond^{TM}-N^{+}, GE Healthcare). Labelling of the *COG6*-specific probe (10 ng), amplified with primers COG6-F4 and COG6-R2 or the β-actin probe (10 ng; Roche), was carried out with the 'random prime labelling system' (GE Healthcare) after addition of [α-^{32}P]dCTP (3000 Ci/mmol; Perkin Elmer) by adhering the manufacturer's guidelines. Hybridization in Amersham Rapid-hyb^{TM} Buffer (GE Healthcare) was accomplished at 70°C for 2 h. Washing of the blot was performed in 2× SSC [0.3 M NaCl, 0.03 M Na_3-citrate with 0.1% (w/v) SDS at 74°C for 20 min and 2× 15 min in 0.2× SSC with 0.1% (w/v) SDS at 65°C], followed by exposure to an autoradiography film.

Retroviral complementation

Ecotropic FNX-Eco cells (5×10^5) were seeded onto dishes (60-mm diameter) 1 day before transfection. Transient transfection by FuGENE6 reagent was performed according to the manufacturer's protocol (Roche), with 1 μg of LNCX2 vector (mock), and LNCX2 with the wild-type *COG6*-cDNA. Further procedures were performed as described elsewhere (28). The supernatant with the amphotropic retroviral particles was used to transfect patient and control fibroblasts. After infection of fibroblasts, the medium was replaced by DMEM, containing 10% heat-inactivated FCS with 225 μg/ml G418 (Gibco BRL). Selection was carried out for 10 days.

Table 2. Primers for *COG5* to *COG8* amplifications and sequencing

Gene	Primer	Sequence (5′ → 3′)
COG5	COG5-F1	CCAGGCGCGGGCTGAGAG
(cDNA)	COG5-F2	GCCAGGTGGGCCTGGAGC
	COG5-F3	GTCGTTGGAAGGTGTTCTTCAG
	COG5-F4	CTCAAGTCGGAACAGCTCTTC
	COG5-F5	CTCACTACAACCCTATGAGGC
	COG5-R1	GCTAAAGAGGTAAATAAACGTCG
	COG5-R2	CCAACTATGAATGGGTTAGCAC
COG6	COG6-Ex2-F1	GTTAGCAGACTCGTTAAAGACAA
(exon 2)	COG6-Ex2-F2	GTTACTAATATATAAAGTAGATATGTA
	COG6-Ex2-R1	GTGCCACTGCACTCCAGCC
	COG6-Ex2-R2	GAAATGGAACAATATAGCAAATTAG
COG6	COG6-F1	GGTCCCTGCCTGGCTGAGG
(cDNA)	COG6-F2	GAGGTGGCAGCAGGGGGC
	COG6-F3	GACAAGTCGCCTACAGGCAG
	COG6-F4	GATGGCCTTACTTCAAGAAACG
	COG6-F5	GTGGTATTGTTGGAAATAGTGC
	COG6-R1	CTTACTTCCCTGTTACTGAGAC
	COG6-R2	CCTTCAGTGTTTTAGGGAGGTC
COG7	COG7-F1	GCCTCGGTGCTCTCGCAGG
(cDNA)	COG7-F2	GTTCTGGACGCCAGGCCTGA
	COG7-F3	GCAGATAAGTGGAGCACGTTGA
	COG7-F4	GGAGCTGGTGGATGCTGTGTA
	COG7-F5	GCAACCACAACCTGCTGGCT
	COG7-R1	CTGCCCAATCTTGGGCAGAGT
	COG7-R2	CAGCCCTGGCTCTCTTG
COG8	COG8-F1	GTTCGGAGTCAGCGCCCCTTGT
(cDNA)	COG8-F2	GGTCCGGAAGGGAAGTGACG
	COG8-F3	CGTGGAGGCGTCGCTCGG
	COG8-F4	CGAGATGCTTGGCTCCGGTC
	COG8-F5	CCTGTTTTCCAGCGGGTGGC
	COG8-R1	CCATCTCGTGCTGGATGATGC
	COG8-R2	CCTGTTCTCCATTGGGGTCC

Gel filtration chromatography

Control and patient-derived fibroblasts were lysed in PBS complemented with 1× protease inhibitor mix (Serva) and 0.75% 3-[(3-cholamido-propyl)dimethylammonium]-1-propanesulfonate by passing 20 times through a dounce homogenizer. After centrifugation at 100 000*g* and 4°C for 30 min, the supernatant was removed and put on ice. The protein concentration of the supernatant was adjusted to 8 mg protein in 400 μl PBS and fractionated over a Superose 6 10/300 GL gel filtration column (GE Healthcare) by FPLC in PBS with a flowrate of 0.25 ml/min for 96 min. For precipitation, each fraction was filled with four volumes of ice-cold acetone and incubated overnight at −20°C. Proteins of each fraction were pelleted by centrifugation at 13000 rpm and 4°C for 15 min, washed with 50% acetone/H_2O and analysed by western blot with an antibody against COG4. Marker proteins thyroglobulin, ferritin and aldolase were purchased from GE Healthcare (Gel Filtration Calibration Kit).

BFA assay

Cells from a control and our patient were grown on glass cover slips for 16 h. After removal of the medium, pre-heated DMEM containing 10% FCS/50 IU/ml penicillin and 50 μg/ml streptomycin/2.5 μg/ml BFA was added to the plate, followed by incubation for 0–15 min at 37°C and 5% CO_2. Incubation was terminated by putting the cells on ice, rinsed twice with ice-cold PBS and fixed with 3% paraformaldehyde for 20 min. After washing the cover slips twice with PBS, free aldehyde groups were blocked with 50 mM NH_4Cl in PBS for 10 min and the cells were permeabilized with 0.5% Triton X-100. Subsequently, the cells were incubated with antibodies against GM130 for 1 h at 37°C, washed with PBS, and then incubated with 10% goat serum in PBS for 20 min. Primary antibodies were detected by secondary antibodies conjugated to the fluorochromes Alexa488. After washing with PBS, the cells were mounted in Vectashield mounting medium with DAPI and analysed using a spinning disk confocal laser microscope (ERS6; Perkin Elmer). Quantification of the ER staining pattern was performed in control and patient-derived fibroblasts by analysing 300 cells each after BFA treatment at different time points.

Conflict of Interest statement. None declared.

FUNDING

This work was supported by a grant of the Deutsche Forschungsgemeinschaft (KO2152/2-2) to C.K.

REFERENCES

1. Dube, D.H. and Bertozzi, C.R. (2005) Glycans in cancer and inflammation-potential for therapeutics and diagnostics. *Nat. Rev. Drug. Discov.*, **4**, 477–488.
2. Moskal, J.R., Kroes, R.A. and Dawson, G. (2009) The glycobiology of brain tumors: disease relevance and therapeutic potential. *Expert. Rev. Neurother.*, **9**, 1529–1545.
3. Schachter, H. and Freeze, H.H. (2009) Glycosylation diseases: quo vadis? *Biochim. Biophys. Acta*, **1792**, 925–930.
4. Haeuptle, M.A. and Hennet, T. (2009) Congenital disorders of glycosylation: an update on defects affecting the biosynthesis of dolichol-linked oligosaccharides. *Hum. Mutat.*, **30**, 1628–1641.
5. Rind, N., Schmeiser, V., Thiel, C., Absmanner, B., Lübbehusen, J., Hocks, J., Apeshiotis, N., Wilichowski, E., Lehle, L. and Körner, C. (2010) A severe human metabolic disease caused by deficiency of the endoplasmatic mannosyltransferase hALG11 leads to congenital disorder of glycosylation-Ip. *Hum. Mol. Genet.*, **19**, 1413–1424.
6. Foulquier, F. (2009) COG defects, birth and rise! *Biochim. Biophys. Acta*, **1792**, 896–902.
7. Reynders, E., Foulquier, F., Leão Teles, E., Quelhas, D., Morelle, W., Rabouille, C., Annaert, W. and Matthijs, G. (2009) Golgi function and dysfunction in the first COG4-deficient CDG type II patient. *Hum. Mol. Genet.*, **18**, 3244–3256.
8. Paesold-Burda, P., Maag, C., Troxler, H., Foulquier, F., Kleinert, P., Schnabel, S., Baumgartner, M. and Hennet, T. (2009) Deficiency in COG5 causes a moderate form of congenital disorders of glycosylation. *Hum. Mol. Genet.*, **18**, 4350–4356.
9. Ungar, D., Oka, T., Krieger, M. and Hughson, F.M. (2006) Retrograde transport on the COG railway. *Trends. Cell. Biol.*, **16**, 113–120.
10. Shestakova, A., Zolov, S. and Lupashin, V. (2006) COG complex-mediated recycling of Golgi glycosyltransferases is essential for normal protein glycosylation. *Traffic*, **7**, 191–204.
11. Oka, T., Ungar, D., Hughson, F.M. and Krieger, M. (2004) The COG and COPI complexes interact to control the abundance of GEARs, a subset of Golgi integral membrane proteins. *Mol. Biol. Cell.*, **15**, 2423–2435.
12. Wu, X., Steet, R.A., Bohorov, O., Bakker, J., Newell, J., Krieger, M., Spaapen, L., Kornfeld, S. and Freeze, H.H. (2004) Mutation of the COG complex subunit gene COG7 causes a lethal congenital disorder. *Nat. Med.*, **10**, 518–523.
13. Foulquier, F., Vasile, E., Schollen, E., Callewaert, N., Raemaekers, T., Quelhas, D., Jaeken, J., Mills, P., Winchester, B., Krieger, M. *et al.* (2006) Conserved oligomeric Golgi complex subunit 1 deficiency reveals a

previously uncharacterized congenital disorder of glycosylation type II. *Proc. Natl Acad. Sci. USA*, **103**, 3764–3769.
14. Foulquier, F., Ungar, D., Reynders, E., Zeevaert, R., Mills, P., García-Silva, M.T., Briones, P., Winchester, B., Morelle, W., Krieger, M. *et al.* (2007) A new inborn error of glycosylation due to a Cog8 deficiency reveals a critical role for the Cog1-Cog8 interaction in COG complex formation. *Hum. Mol. Genet.*, **16**, 717–730.
15. Kranz, C., Ng, B.G., Sun, L., Sharma, V., Eklund, E.A., Miura, Y., Ungar, D., Lupashin, V., Winkel, R.D., Cipollo, J.F. *et al.* (2007) COG8 deficiency causes new congenital disorder of glycosylation type IIh. *Hum. Mol. Genet*, **16**, 731–741.
16. Lippincott-Schwartz, J., Yuan, L.C., Bonifacino, J.S. and Klausner, R.D. (1989) Rapid redistribution of Golgi proteins into the ER in cells treated with Brefeldin A: evidence for membrane cycling from Golgi to ER. *Cell*, **56**, 801–813.
17. Oka, T., Vasile, E., Penman, M., Novina, C.D., Dykxhoorn, D.M., Ungar, D., Hughson, F.M. and Krieger, M. (2005) Genetic analysis of the subunit organization and function of the conserved oligomeric Golgi (COG) complex: studies of COG5- and COG7-deficient mammalian cells. *J. Biol. Chem.*, **280**, 32736–32745.
18. Steet, R. and Kornfeld, R. (2006) COG-7-deficient human fibroblasts exhibit altered recycling of Golgi proteins. *Mol. Biol. Cell*, **17**, 2312–2321.
19. Whyte, J.R. and Munro, S. (2001) The Sec34/35 Golgi transport complex is related to the exocyst, defining a family of complexes involved in multiple steps of membrane traffic. *Dev. Cell.*, **1**, 527–537.
20. Ram, R.J., Li, B. and Kaiser, C.A. (2002) Identification of Sec36p, Sec37p, and Sec38p: components of yeast complex that contains Sec34p and Sec35p. *Mol. Biol. Cell*, **13**, 1484–1500.
21. Niehues, R., Hasilik, M., Alton, G., Körner, C., Schiebe-Sukumar, M., Koch, H.G., Zimmer, K.P., Wu, R., Harms, E., Reiter, K. *et al.* (1998) Carbohydrate-deficient glycoprotein syndrome type 1b: phosphomannose isomerase deficiency and mannose therapy. *J. Clin. Invest.*, **101**, 1414–1420.
22. Fang, J., Peters, V., Assmann, B., Körner, C. and Hoffmann, G.F. (2004) Improvement of CDG diagnosis by combined examination of several glycoproteins. *J. Inherit. Metab. Dis.*, **27**, 581–590.
23. Wopereis, S., Grünewald, S., Morava, E., Penzien, J.M., Briones, P., Garcia Silva, M.T., Demacker, P.N., Huijben, K.M. and Wevers, R.A. (2003) Apolipoprotein C-III isofocusing in the diagnosis of genetic defects in O-glycan biosynthesis. *Clin. Chem.*, **49**, 1839–1845.
24. Hansske, B., Thiel, C., Lübke, T., Hasilik, M., Höning, S., Peters, V., Heidemann, P.H., Hoffmann, G.F., Berger, E.G., von Figura, K. *et al.* (2002) Deficiency of UDP-galactose:*N*-acetylglucosamine beta-1,4-galactosyltransferase I causes the congenital disorder of glycosylation type IId. *J. Clin. Invest.*, **109**, 725–733.
25. Lübke, T., Marquardt, T., Etzioni, A., Hartmann, E., von Figura, K. and Körner, C. (2001) Complementation cloning identifies CDG-IIc, a new type of congenital disorders of glycosylation, as a GDP-fucose transporter deficiency. *Nat. Genet.*, **28**, 73–76.
26. Lübke, T., Marquardt, T., von Figura, K. and Körner, C. (1999) A new type of carbohydrate deficient glycoprotein syndrome due to a decreased import of GDP-fucose into the Golgi. *J. Biol. Chem.*, **274**, 25986–25989.
27. Sambrook, J. and Russel, D.W. (2001) *Molecular Cloning: A Laboratory Manual*. Cold Spring Harbour Laboratory Press, Cold Spring Harbour, NY.
28. Thiel, C., Schwarz, M., Hasilik, M., Grieben, U., Hanefeld, F., Lehle, L., von Figura, K. and Körner, C. (2002) Congenital disorder of glycosylation-Ig is caused by deficiency of dolichyl-P-Man:$Man_7GlcNAc_2$-PP-dolichyl mannosyltransferase. *Biochem. J.*, **367**, 195–201.